JOURNAL OF NEUROTRAUMA 32:1031–1045 (July 15, 2015)

DOI: 10.1089/neu.2014.3610

Original Articles

Resting State Functional Connectivity in Mild Traumatic Brain Injury at the Acute Stage: Independent Component and Seed-Based Analyses

Armin Iraji,[1] Randall R. Benson,[2] Robert D. Welch,[3] Brian J. O'Neil,[3] John L. Woodard,[4] Syed Imran Ayaz,[3] Andrew Kulek,[3] Valerie Mika,[1,3] Patrick Medado,[3] Hamid Soltanian-Zadeh,[5] Tianming Liu,[6] E. Mark Haacke,[1,7] and Zhifeng Kou[1,7]

Abstract

Mild traumatic brain injury (mTBI) accounts for more than 1 million emergency visits each year. Most of the injured stay in the emergency department for a few hours and are discharged home without a specific follow-up plan because of their negative clinical structural imaging. Advanced magnetic resonance imaging (MRI), particularly functional MRI (fMRI), has been reported as being sensitive to functional disturbances after brain injury. In this study, a cohort of 12 patients with mTBI were prospectively recruited from the emergency department of our local Level-1 trauma center for an advanced MRI scan at the acute stage. Sixteen age- and sex-matched controls were also recruited for comparison. Both group-based and individual-based independent component analysis of resting-state fMRI (rsfMRI) demonstrated reduced functional connectivity in both posterior cingulate cortex (PCC) and precuneus regions in comparison with controls, which is part of the default mode network (DMN). Further seed-based analysis confirmed reduced functional connectivity in these two regions and also demonstrated increased connectivity between these regions and other regions of the brain in mTBI. Seed-based analysis using the thalamus, hippocampus, and amygdala regions further demonstrated increased functional connectivity between these regions and other regions of the brain, particularly in the frontal lobe, in mTBI. Our data demonstrate alterations of multiple brain networks at the resting state, particularly increased functional connectivity in the frontal lobe, in response to brain concussion at the acute stage. Resting-state functional connectivity of the DMN could serve as a potential biomarker for improved detection of mTBI in the acute setting.

Key words: functional connectivity; fMRI; functional MRI; mTBI; mild traumatic brain injury; resting state fMRI

Introduction

Traumatic brain injury (TBI) is a significant public health burden in the United States and worldwide.[1,2] Most patients with mTBI experience an injury of mild severity, often referred to as mild TBI (mTBI),[3] accounting for more than 1 million emergency department (ED) visits annually in the United States.[4] Most patients with mTBI usually stay in the EDs only for a few hours and then are discharged home without specific follow-up instructions, which is surprising given that a number of patients with mTBI experience acute and protracted neurocognitive symptoms. Further, even a mild injury can have a substantial impact on their quality of life and society.[3,5,6] Such rapid ED discharge is based on negative CT findings for most patients with mTBI.

The acute setting is a golden window of opportunity for impacting current treatment of patients with mTBI.[7] A constant challenge for emergency physicians is to detect neural abnormalities in patients with mTBI that may impact patients' protracted recovery or prolonged neurocognitive symptoms,[7] which may hold the best opportunity to improve the proactive treatment of patients with mTBI.

Advanced magnetic resonance imaging (MRI) holds great potential for mTBI injury detection and outcome prediction.[8,9] Examples include diffusion tensor imaging (DTI),[10–19] susceptibility weighted imaging (SWI),[20–22] perfusion imaging, and MR spectroscopy, among others.[8,9] Clinical and neurocognitive features of patients with mTBI include attention and memory deficits among a constellation of other physical and emotional symptoms. Given the

[1]Department of Biomedical Engineering, Wayne State University, Detroit, Michigan. [2]Center for Neurologic Studies, Novi, Michigan.
[3]Department of Emergency Medicine, Wayne State University, Detroit, Michigan.
[4]Department of Psychology, Wayne State University, Detroit, Michigan.
[5]Department of Radiology, Henry Ford Hospital, Detroit, Michigan.
[6]Department of Computer Science, University of Georgia, Athens, Georgia.
[7]Department of Radiology, Wayne State University, Detroit, Michigan.

fact that most patients with mTBI have no obvious damage on structural MRI, functional MRI (fMRI) may be a viable alternative for detecting injury-related abnormalities.[23–26]

Resting-state fMRI (rsfMRI), which reflects brain activity at rest while not performing any specific task, could reveal possible disruption in cognitive function from mild TBI.[27,28] rsfMRI has the advantage of detecting abnormalities in functional connectivity (FC) even in the presence of unremarkable structural imaging results. Numerous studies have reported disruptions of the resting-state networks (RSNs) and the brain's intrinsic low FC in various disorders, such as Alzheimer disease (AD), schizophrenia, attention deficit hyperactivity disorder (ADHD), and mTBI.[27–31]

Among all brain networks at the resting state, the Default Mode Network (DMN) is the most widely studied network in mTBI.[27,28,32,33] The DMN is assumed to control passive mental activities while persons are awake and alert but do not specifically perform any goal-directed task.[34] The posterior cingulate cortex (PCC) and the medial prefrontal cortex (MPFC) are two important components of the DMN. The PCC and MPFC are associated with self-referential and emotional processing, as well as semantic processing,[35] and their activity is attenuated when attention to a goal-directed task increases.[36] The reported important role of the DMN in several cognitive functions and its disruption in several neurocognitive disorders both highlight the importance of the connections of the DMN and possible alterations in its activity as a possible diagnostic marker of injury-related neural damage.

In terms of analysis of rsfMRI data, seed-based region of interest (ROI) analysis, also called seed-based analysis (SBA), is widely used. Mayer and associates[27] studied patients with mTBI at the subacute stage (within 2 weeks after injury) by choosing the rostral anterior cingulate gyrus as the seed region and demonstrated a reduction in connectivity within the DMN for patients with mTBI and an increase in connectivity within a task-related network (TRN) relative to matched controls. Similarly, Johnson and colleagues[28] scanned sports athletes with mTBI at the subacute phase (10 ± 2 days). By using both voxel-based and ROI-based analysis, they focused on DMN regions such as the PCC, MPFC, lateral parietal lobes, and the parahippocampal gyrus. They indicated that both the number and strength of connections decreased in the PCC and the lateral parietal cortices but increased in the MPFC.

For ICA analysis, Stevens and coworkers[32] explored different independent components analysis (ICA) components to find alterations between healthy subjects and patients with mTBI who underwent scanning 61 days after injury. They found diminished FC in the patient group in the DMN and many other networks, such as the primary visual processing circuit, the motor system, the left-lateralized frontoparietal circuit, the dorsomedial circuit, the frontoparietal executive system, and the frontostriatal network. They also found that the precuneus has greater connectivity with the DMN, while the connectivity between the cingulate and this network decreases.

Tang and colleagues[37] explored alterations in thalamus connectivity for patients with mTBI with a 22-day mean interval after injury. The thalamus contributes to communication between various cortical regions of the brain. In the seed-based method, the patients with mTBI demonstrated more widely distributed FC between thalamic and cortical regions. The ICA analysis indicated an increase in thalamocortical functional connectivity at the posterior cingulate and frontal regions in patients compared with healthy control subjects. They suggested an up-regulation of thalamocortical FC in response to disruption of thalamic RSNs in patients with mTBI.[37]

To date, most studies were conducted during the subacute or chronic stage, given that patients with mTBI were imaged between 10 and 60.9 days after injury or even longer. Few studies have investigated the alterations of RSN in mTBI at the acute stage, which is within 24 h post-injury or sooner. This time frame corresponds to the maximum amount of time that patients with mTBI typically stay within EDs, and rapid treatment of patients within this time frame can have a direct impact on their acute care.[7]

In addition, it is at the acute stage that most patients with mTBI report post-concussion symptoms (PCS) and neurocognitive problems. Although approximately 50% of patients' clinical and neurocognitive symptoms resolve during the subacute stage and most patients' symptoms have resolved by the chronic stage,[38] some patients with mTBI experience protracted symptoms. Detection of the neural basis of brain injury at the acute stage will be most likely to shed light on the link between early functional abnormalities and the possibility of protracted symptoms.

In addition to alterations in the DMN and thalamus connectivity, memory problems are one of the most prevalent neurocognitive symptoms experienced at the acute stage, in suggestion of likely disruption of the hippocampal functional networks.[39] In addition, emotional and behavioral symptoms in mTBI also suggest involvement of the limbic network, involving the amygdala. Along with the fusiform gyrus, the hippocampus is vulnerable because of its position within the middle cranial fossa and petrous bone, a region likely to directly sustain deformation injury, which in turn could affect connectivity. This also explains the functional network alterations seen when using the parahippocampal gyrus as a seed region as reported by Johnson and coworkers.[28]

In addition, the trauma incident is also an emotional event, as well as causing physical or physiological disruptions of the brain. Emotional disturbances such as anxiety and depression immediately after mTBI in the acute setting also suggest that the amygdala may play a role as well. Because of the location of the sphenoid bone in conjunction with the tentorium cerebelli, the amygdala is highly likely to be injured at all levels of injury severity, including mild.

In this prospective study, we have investigated RSNs in patients with mTBI and have assessed their clinical and neurocognitive symptoms within 24 h while they are still either at the ED or in the hospital. We used both ICA and ROI analyses by looking at both the DMN and thalamic regions as well as the hippocampus and amygdala to determine group differences between patients and controls. Our objective is to identify a possible neural basis of acute clinical and cognitive symptoms in mTBI by using rsfMRI. We hypothesized that the brain may demonstrate altered functional connectivity in the DMN and networks involving the thalamus, hippocampus, and amygdala in response to brain injury at the acute stage.

Methods

Subject recruitment

This study was approved by both the Human Investigation Committee of Wayne State University and the Institutional Review Board of Detroit Medical Center. Written informed consent was obtained from each subject before enrollment. All subjects were at least 18 years old and able to speak English. All patients with mTBI were recruited from the ED of Detroit Receiving Hospital (DRH), which is a Level-I trauma center. Patient eligibility was based on the mTBI definition by the American Congress of Rehabilitation Medicine.[40]

Only patients with a lowest-recorded Glasgow Coma Score (GCS) of 13–15 were considered. For a GCS of 15, there must be least one of the following: (a) loss of consciousness less than

30 min, (b) post-traumatic amnesia less than 24 h, or (c) an alteration in mental status (i.e., disoriented, dazed, or confused). Participants, both healthy controls and patients, with a history of a previous brain injury, neurological, neuropsychological, or psychiatric disorder, or concurrent substance abuse were excluded. Moreover, MRI exclusion criteria include metal and/or electronic implants, claustrophobia, pregnant or trying to become pregnant, and subjects weighing more than 300 pounds (136 kg; machine's capacity limit). If the MRI scan could not be performed in the acute setting in a patient, the patient was brought back for an MRI scan within a week of injury.

Cognitive assessment

In the acute setting, once a patient was conscious and medically stable and came out of post-traumatic amnesia, if any, they would be administered neurocognitive testing and surveyed about their PCS. A short instrument called the Standardized Assessment of Concussion (SAC)[41] was used as a brief assessment of neurocognitive function. The SAC was originally developed for field assessment of neurocognitive status after a sports concussion.[42] It has been reported that the SAC is sensitive to the acute changes after concussion and requires limited training to administer.[39]

The SAC is scored 0 to 30 and assesses four cognitive domains including orientation, attention, immediate memory, and delayed recall. The SAC has demonstrated sensitivity to brain injury in the acute setting, particularly in delayed recall.[39] The Emergency Room Edition of the SAC also includes a PCS questionnaire where symptoms were graded from 0 to 3 (i.e., none, mild, moderate, severe). The PCS score was the sum of symptom scores for the questionnaire.

Image acquisition

MRI data were collected on a 3-Tesla Siemens Verio scanner with a 32-channel radiofrequency head-only coil. A subject's head was fixed by foam pads to restrict motion. Resting state functional imaging was performed using a gradient echo echo-planar imaging sequence with the following imaging parameters: repetition time (TR) = 2000 msec, echo time (TE) = 30 msec, slice thickness = 3.5 mm, slice gap = 0.595 mm, flip angle = 90 degrees, pixel size = 3.125 mm in-plane, matrix size = 64 × 64, 240 volumes for whole-brain coverage, one average, acquisition time of 8 min. During resting-state scans, subjects were instructed to keep their eyes closed and to stay awake. In addition, structural high-resolution T1-weighted imaging was also performed by using the MPRAGE sequence with TR = 1950 ms, TE = 2.26 ms, slice thickness = 1 mm, flip angle = 9 degrees, field of view = 256 × 256 mm, matrix size = 256 × 256, and voxel size = 1 mm isotropic.

Image processing

Figure 1 demonstrates a pipeline of the comprehensive image processing. We used both ICA and SBA to analyze the resting state fMRI (rsfMRI). ICA was performed at both group and individual levels. Group ICA was performed first in both patient and control groups and then with cross-validation in subgroups. Individual ICA was performed by using two reported methods, ''dual regression''[43,44] and ''back-projection,''[43,44] and our new atlas-based ICA method to overcome the confounding factors of these two methods. ICA analysis was mainly performed in DMN and the basal ganglia network (BGN). Because the thalamus belongs to BGN, which is an independent network in ICA analysis in published data,[45] we investigated BGN to assess the thalamus in the ICA analysis.

After ICA analysis, SBA was also performed by calculating the Pearson correlation value between major network regions and the whole brain, and the correlation maps were used to compare healthy controls and patients. The network regions were selected for DMN, BGN, amygdala and hippocampus regions based on previous studies.[27,28,37] Specifically, the PCC, precuneus, angular, anterior prefrontal cortex (Brodmann area [BA] 10), and orbitofrontal cortex (BA 11) were selected for the DMN; and the putamen, pallidum, thalamus, and caudate were selected for the BGN. Below is a description of major steps.

Preprocessing. Preprocessing was performed using the FSL software (http://www.fmrib.ox.ac.uk/fsl/). First, the first five volumes were discarded to reach magnetization equilibrium. A high-pass temporal filtering (100 sec), motion correction, slice timing, brain extraction, and spatial smoothing (full width at half maximum = 6 mm) were applied. Grand mean scaling was also applied to the entire 4-dimensional data for each subject. The data were registered to the Montreal Neurological Institute standard space using nonlinear registration with 10 mm warp resolution and resampled to 3 mm isotropic voxel size. Variance normalization was used to rescale each time series. No intensity normalization was performed to prevent false anticorrelation. In addition, for SBA, the white matter (WM) and cerebrospinal fluid (CSF) signal were regressed out using the DPARSF toolbox (http://www.restfmri.net/forum/DPARSF).

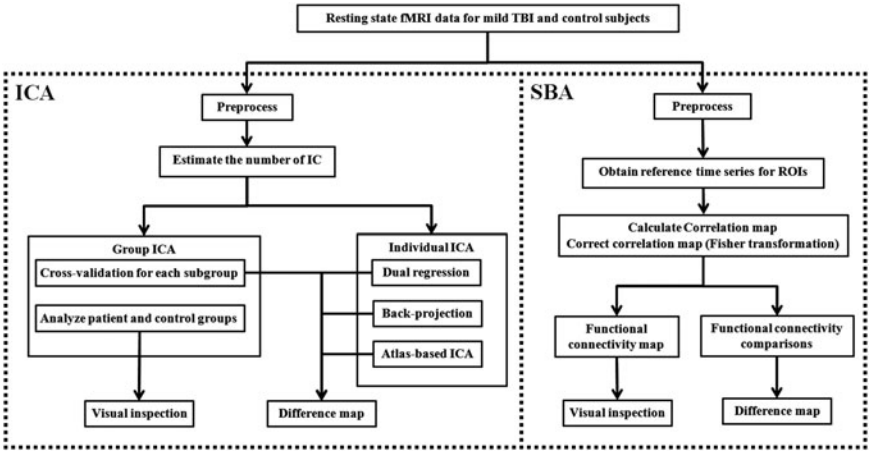

FIG. 1. Image processing pipeline. fMRI, functional magnetic resonance imaging; TBI, traumatic brain injury; ICA, independent component analysis; SBA, seed-based analysis; ROI, region of interest.

Group ICA (GICA) analysis. ICA was performed using the GIFT software package from MIALAB (http://mialab.mrn.org/software/gift/) and the MELODIC package, which is included in FSL (http://www.fmrib.ox.ac.uk/fsl/melodic). We chose 52 components for our analysis and applied an automated two-step approach for network selection to eliminate human errors (see Supplement 1 for further explanations; see online supplementary material at ftp.liebertpub.com). Briefly, the DMN and BGN were determined by using the spatial correlation similarity metric (Eq. 1) between ICA components and a template of the desired RSNs. The template includes 75 components built by Allen and coworkers[45] based on 603 subjects that contains 28 RSNs (see Supplement 1 for further explanations; see online supplementary material at ftp .liebertpub.com).

$$r = \frac{\sum_i X_i Y_i}{\sqrt{\sum_i X_i^2 \times \sum_i Y_i^2}}, \qquad \text{Eq. 1}$$

Where i is the number of voxels, X is a desired RSN, and Y is a component obtained from ICA.

The GICA was performed on the healthy control and patient groups. The group difference was measured between patients and controls in major network regions of both the DMN and BGN. The reliability and reproducibility of the results were measured by using a cross-validation method. Specifically, for each group (patient or healthy control), seven subgroups were randomly chosen with six subjects in each subgroup. GICA was performed for each subgroup, and the number of voxels in each network region associated with the related network and the voxel dependency were measured. Voxel dependency is a voxel's value of RSN map (the result of ICA) indicating its likelihood of belonging to the network—in other words, the extent to which a voxel belongs to the network.

Individual ICA. Individual ICA was performed using two reported methods—i.e., dual regression[43,44] and back-projection,[43,44] as well as a new atlas-based ICA approach to evaluate the alterations in patients with mTBI. The common space in both ICA methods was created by using the whole dataset of this study, because extracting the independent components of each group separately may overestimate the difference between groups. Given the relative small sample size in this study, however, the common space may still be different from that of the normal population. To overcome the potential confounding factor, we proposed an atlas-based ICA method.

Proposed atlas-based ICA. In the atlas-based ICA, independent components extracted from 603 subjects[45] were used as the common space, and a ''spatially constrained ICA'' method[46] was used to extract the individual components corresponding to the common space components.

Because the common space in the dual regression and back-projection methods is created by using the whole dataset of a particular study, the common spaces are different when the datasets of studies differ from each other. Consequently, RSNs of an individual could be changed depending on the group to which the individual belongs. On the other hand, in the temporal concatenation group ICA, we assume that there is a common space among all individuals; therefore, using the data of a study to find the common space is not ideal, especially when the number of samples is small, as in our study. Therefore, a template or atlas that indicates the common space of a big population is needed.

In the atlas-based ICA, unlike the dual regression and back-projection, instead of using the independent components of GICA of our dataset as a common space for individual ICA, the independent components from a large group of healthy subjects are considered as a true common space. In this case, (1) the RSNs extracted from an individual's rsfMRI data are more reliable because independent components were extracted from an atlas that is based on a large population instead of a small group of subjects; (2) independent components and subsequent analysis and results among various studies with different data sets only depend on individual differences rather than the whole data set in an study, because the common space is the same among all of this study. In other words, the difference between various subjects is only the result of the intrinsic variability between each pair of them.

Note that because this method uses atlas components to extract the individual components in individual subjects, it automatically solves the problem of finding corresponding RSNs across subjects. As previously explained, this method only requires the individual subject's data instead of a whole set of subjects' data, which makes it more applicable for clinical use.

SBA. SBA was performed using within-group and between-group analyses. A Pearson correlation coefficient was determined between the average of all voxels in a network region and all brain voxels to create a correlation map for each region.[37] The correlation maps were corrected by using the Fisher z-transformation to calculate a FC map and FC comparisons. The FC map was calculated by applying a one-sample t test on corrected correlation maps. In FC comparisons, a correlation mask was first applied to select voxels that are eligible for statistical analysis (see Supplement 1 for details regarding SBA; see online supplementary material at ftp.liebertpub.com). Then, statistical analysis was performed using two-sample t tests on corrected correlation maps that were further corrected by spatial thresholding to reduce the false positives and increase reliability.

Statistical analysis

Statistical analysis was performed using MATLAB software (http://www.mathworks.com/). Data normality was assessed by using the Kolmogorov–Smirnov test. Results for continuous variables are presented as mean (standard deviation [SD]) or median (interquartile range) as appropriate. Frequencies and percentages are presented for categorical variables. Unless specifically stated otherwise, a p value < 0.05 was considered significant. For ICA, a two-sample t test was performed to compare RSNs between two groups when appropriate. For SBA, the correlation value was converted using the Fisher z-transformation to maintain the statistical analysis eligibility (see Supplement 1 for details; see online supplementary material at ftp.liebertpub.com).

A two-sample t test was performed for FC comparisons, and a one-sample t test was performed to determine the FC map for each network region. Statistical maps for both ICA and SBA were corrected with spatial (cluster) thresholding with the MonteCarlo simulation using Alphasim contained within resting-state fMRI software (http://www.restfmri.net/) to decrease false-positive error. In other words, to correct type I error without increasing the risk of type II error, dual thresholding (based on p value and cluster size) was performed to give a high reliability for statistical results.

Moreover, to increase the reliability of the between-group comparison, the healthy subjects were randomly divided into two groups, and a within-group analysis was performed by using the two-sample t test. The results were compared with the between-group analysis to improve reliability that the difference, which appears in between-group analysis, is generated from the group difference. Finally, the relationship between imaging analyses and the neurocognitive measurements, including SAC scores and scores of each SAC subcategory, were evaluated with bivariate correlations.

Results

Demographic and clinical characteristics are presented in Table 1. In the patient group ($n = 12$), 6 (50%) were men and 6 (50%)

Table 1. Individual Demographic and Clinical Data of the 12 Patients Enrolled in the Study

Group	*Subject ID*	*Age/sex*	*Race*	*Mechanism of injury*	*MRI findings*	*Scan time delay*
Patients	PT-001	56/M	Indian	MVC	WMHI, IVH	26 h
	PT-002	35/M	Black	Fall	Negative	36 h
	PT-003	54/F	Black	MVC	Negative	5 h
	PT-004	31/F	Black	MVC	Negative	12 h
	PT-005	30/M	White	Sport	Negative	7 days
	PT-006	36/F	Black	MVC	Negative	9 h
	PT-007	19/M	Black	MVC	WMHI	3 h
	PT-008	30/F	Asian	MV vs. Ped.	Negative	8 h
	PT-009	51/M	Black	Assault	WMHI	13 h
	PT-010[a]	23/M	Black	MVC	Negative	9 h
	PT-011[a]	21/F	White	MVC	Negative	48 h
	PT-012[a]	73/F	Black	Fall	WMHI	6 h
	Summary	38 ± 17 (Mean ± SD) 6/6 (F/M)				13 h (Median) 3 h–7 days (Range)
Healthy controls	CTRL-001	52/F	White	N/A	Negative	N/A
	CTRL-002	44/M	White	N/A	WMHI	N/A
	CTRL-003	41/M	White	N/A	Negative	N/A
	CTRL-004	28/F	White	N/A	Negative	N/A
	CTRL-005[a]	27/F	White	N/A	Negative	N/A
	CTRL-006	29/M	Middle East	N/A	Negative	N/A
	CTRL-007	33/M	White	N/A	Negative	N/A
	CTRL-008	24/F	Asian	N/A	Negative	N/A
	CTRL-009	23/M	Indian	N/A	Negative	N/A
	CTRL-010	45/M	White	N/A	Negative	N/A
	CTRL-011	22/M	White	N/A	Negative	N/A
	CTRL-012	27/M	Asian	N/A	Negative	N/A
	CTRL-013	23/F	Asian	N/A	Negative	N/A
	CTRL-014	22/F	Asian	N/A	Negative	N/A
	CTRL-015	65/F	Asian	N/A	Negative	N/A
	CTRL-016	23/M	White	N/A	Negative	N/A
	Summary	33 ± 13 (Mean ± SD) 7/9 (F/M)				

MRI, magnetic resonance imaging; MVC, motor vehicle collision; WMHI, white matter hyperintensity; IVH, intraventricular hemorrhage; SD, standard deviation.

[a]Eliminated because of motion artifacts on their images.

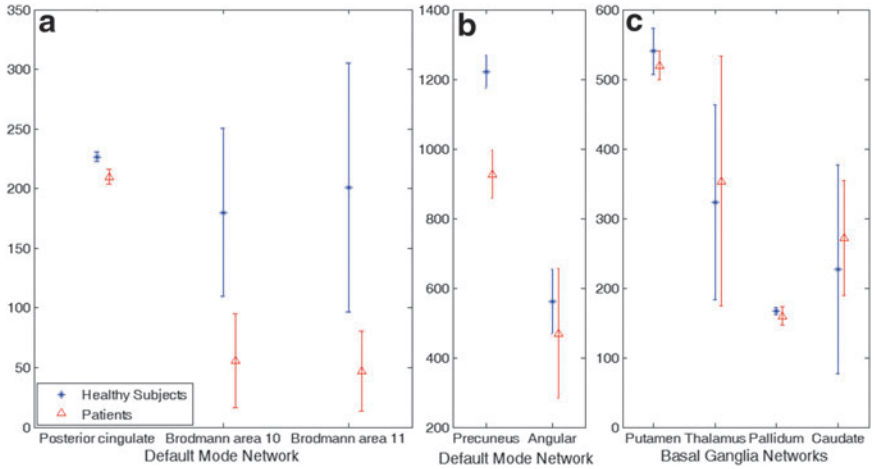

FIG. 2. Cross-validation results of the group independent component analysis on number of associated voxels to the resting state networks. The default mode network shows a difference between the two groups in (**a**) the posterior cingulate cortex, Brodmann area (BA) 10, BA 11 and (**b**) precuneus. (**c**) The basal ganglia network does not show any significant difference. Error bar is one standard deviation. Color image is available online at www.liebertpub.com/neu

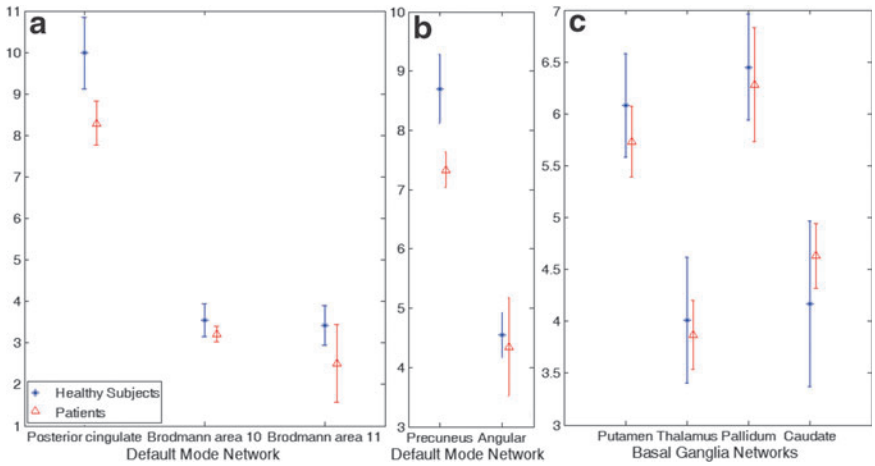

FIG. 3. Cross validation results of the group independent component analysis on voxel dependency to the resting-state networks. The default mode network shows a difference between the two groups in the (**a**) posterior cingulate cortex and (**b**) precuneus. (**c**) The The basal ganglia network does not show any significant difference. Error bar is one standard deviation. Color image is available online at www.liebertpub.com/neu

women. Their age was 38 ± 17 (mean ± standard deviation) years, and GCS scores were all 15 on admission to the ED. Mechanisms of injury included: seven motor vehicle accidents, two falls, one pedestrian struck by a car, one assault, and one sports concussion. All patients had negative CT findings that were diagnosed in the emergency setting. Four patients had ''nonspecific WM hyperintensities'' on FLAIR images, and one had a tiny intraventricular hemorrhage.

For the healthy controls ($n = 16$), 9 (56%) were men and 7 (44%) women, and the mean healthy subject age was 33 ± 13 years. There was no significant age or sex difference between patients with mTBI and healthy controls. Patients with mTBI underwent scanning in the acute setting (median of 13 h post-injury, range 5 h to 7 days). Except for the one patient who underwent scanning 7 days after injury, the rest underwent scanning within 48 h after injury. Three patients and one control subject were later eliminated from the study because of strong motion artifacts in the images, with a total of 9 patients and 15 healthy controls included in the final analysis.

Neurocognitive performance

The mean patient SAC score was 24.5 ± 2.3 (mean ± SD). We compared this mean with published normative data of more than 568 subjects[47] (mean ± SD, 26.3 ± 2.2). The patients' mean SAC score was significantly below this published mean score ($t(12) = -2.96$, $p = 0.015$). Among all subcategories of the SAC test, including orientation, immediate memory, concentration, and delayed recall, only delayed recall was significantly lower than published normalized data ($t(12) = -2.90$, $p = 0.016$).

ICA results

GICA. Figure 2 shows a significant decrease in number of associated voxels in the PCC and precuneus regions of the DMN in patients with mTBI compared with controls. Figure 3 further shows significantly decreased dependency of associated voxels in the same regions in patients with mTBI compared with controls. Table 2 further demonstrates results of the voxel-wise two-sample t-test on cross-validation GICA analysis ($p < 0.01$), showing group differences in the precuneus and PCC. The result shows a substantial reduction of voxel dependency to DMN for the precuneus and PCC, by 31.19% and 42.28%, respectively. The overall reduction for DMN is 10.51%.

By applying a two-sample *t* test with a more conservative *p* value of 0.001, cross-validation GICA results identified a cluster of 50 voxels in the PCC and a cluster of 442 voxels in the precuneus that have significantly lower voxel dependency to the DMN in patients compared with healthy control subjects (Fig. 4).

To sum up, our comprehensive GICA analysis demonstrates a consistent difference in PCC and precuneus between groups, suggesting that resting-state connectivity in these regions could discriminate between patients and healthy controls.

For the BGN, the cross-validation GICA did not reveal any changes in either voxel dependency or the number of voxels in the BGN.

Table 2. Results of Voxel-wise Two-sample *T* test on Cross-validation of group Independent Component Analysis

Network	*Region*	*Number of voxels in the region*	*Number of voxels with group difference* ($p < 0.01$)	*% Difference*
DMN	Posterior cingulate cortex (PCC)	246	104	42.28%
	Precuneus	2026	632	31.19%
	Angular	885	0	0%
	Anterior prefrontal cortex (BA 10)	1397	0	0%
	Orbitofrontal cortex (BA 11)	2447	0	0%
	Overall	7001	736	10.51%
BGN	Thalamus	615	0	0%
	Putamen	606	0	0%
	Pallidum	176	0	0%
	Caudate	581	0	0%
	Overall	1978	0	0%

DMN, default mode network; BGN, basal ganglia network.

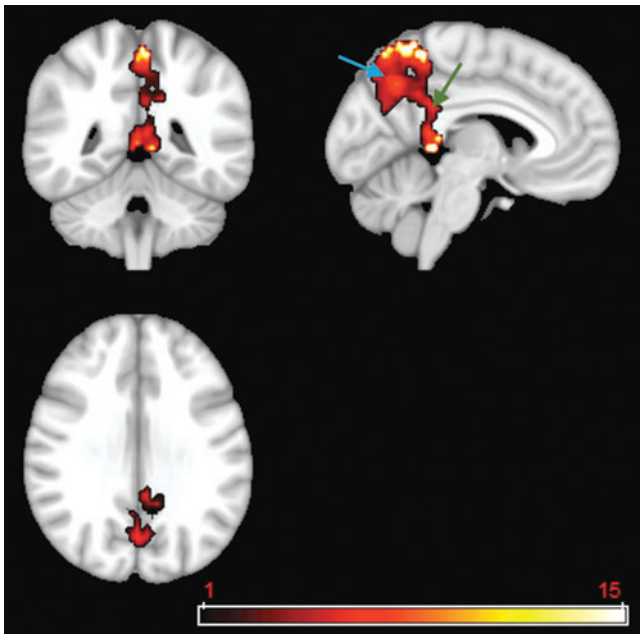

FIG. 4. Two-sample *t* test using a *p* value of 0.001 on the default mode network (DMN) extracted from the cross-validation of group independent component analysis. Results identified a cluster of 50 voxels in the posterior cingulate cortex (green arrow) and a cluster of 442 voxels in the precuneus (blue arrow) that have significantly lower voxel dependency to the DMN in patients compared with healthy control subjects. Color image is available online at www.liebertpub.com/neu

Individual ICA. Individual ICA was performed to investigate alterations of the DMN and BGN in patients compared with healthy controls. Dual regression, back-projection, and the atlas-based spatially constrained ICA have all been applied. Neither dual regression nor back-projection was able to discriminate between the two groups in individual analysis. The atlas-based spatially constrained ICA method, however, demonstrated an intriguing result.

Consistent with GICA results, a two-sample *t* test on the DMNs extracted from the atlas-based ICA method revealed a significant difference between the two groups in the PCC and surrounding areas including the precuneus. For a *p* value = 0.05, the two-sample *t* test map, which was corrected using the spatial threshold, manifested a cluster of 137 voxels with reduced voxel dependency to the DMN in the patient group compared with controls. This includes 55 voxels in the PCC (Fig. 5). This suggests reduced connectivity within the DMN, which is consistent with our GICA results. The ICA results are also consistent with results of Stevens and associates,[32] as discussed above.

SBA

The within-group analysis on healthy controls did not reveal any significant difference; however, the between-group analysis using the same parameters as that of the within-group analysis demonstrated several alterations in patients compared with healthy controls, including in connectivity maps generated by using the PCC, thalamus, amygdala, and hippocampus as seed regions.

PCC connectivity map. Table 3 demonstrates the one-sample *t* test of the FC map generated using the PCC as a seed region. It shows (a) stronger FC between the PCC and the precuneus in the healthy control group than that in patients, which suggests reduced connectivity within the DMN in consistency with the results of ICA; and (b) larger and more distributed FC in different regions of the brain in patients than in the healthy control group (also see supplementary Fig. S1; see online supplementary material at ftp.liebertpub.com). Specifically, patients showed stronger FC between the PCC and the frontal lobe regions than controls (see Table 3 and supplementary Fig. S1; see online supplementary material at ftp.liebertpub.com). For example, the FC map of patients with mTBI using $p = 0.01$ contains clusters with 108 voxels in the dorsolateral prefrontal cortex (BA 9) and 77 voxels in the anterior cingulate cortex (BA 32), while the FC map of the healthy control group does not include any voxels in these two regions. Moreover, the FC map of patients with mTBI contains 262 voxels in the anterior prefrontal cortex (BA 10), compared with the FC map of the healthy control group that has only 59 voxels. (see Table 3 and supplementary Fig. S1; see online supplementary material at ftp.liebertpub.com).

Figure 6 demonstrates further two-sample *t* tests of FC comparison for the PCC map (i.e., using the PCC as a seed region) between patients and controls. It shows significantly higher FC between the PCC and several regions of the frontal lobe in patients compared with controls, including the dorsolateral prefrontal cortex (BA 9) and adjoining voxels in BA 8 and the anterior cingulate cortex (BA 32) (Fig. 6). For *p* value < 0.01, the two-sample *t* test map showed two clusters of 117 and 223 voxels, in the dorsolateral prefrontal cortex (BA 9) with higher FC in patients than in controls. These clusters include 77 and 87 voxels, respectively. Along with a cluster containing 44 voxels in the dorsal anterior cingulate cortex (BA 32), these show the susceptibility of these regions to alterations

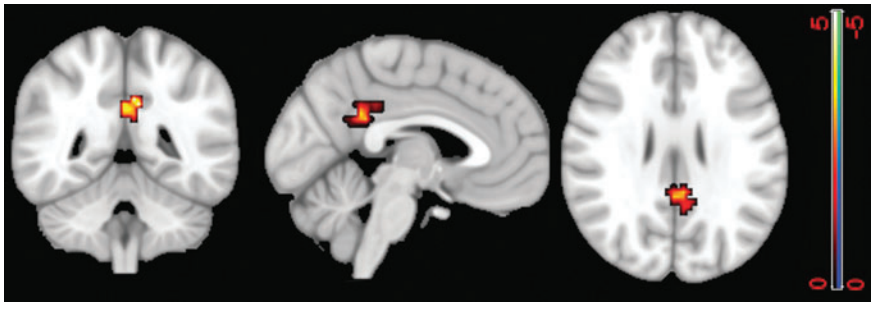

FIG. 5. Two-sample *t* test results demonstrate a difference in the default mode network (DMN) between the two groups in individual independent component analysis. Highlighted area shows the cluster is statistically significant ($p < 0.05$), which includes 55 voxels in the posterior cingulate cortex. The warm color labels the voxels with reduced DMN dependency in patients compared with healthy controls. Color image is available online at www.liebertpub.com/neu

Table 3. One-sample *t* test of the Unctional Connectivity Map Generated using the Posterior Cingulate Cortex as a Seed Region

	Number of voxels with p *value = 0.01*		*Number of voxels with* p *value = 0.001*	
Regions	*Control group*	*Patient group*	*Healthy group*	*Patient group*
Dorsolateral prefrontal cortex (BA 9)	0	108	0	0
Anterior prefrontal cortex (BA 10)	59	262	0	66
Anterior cingulate cortex (BA 32)	0	77	0	15
Cingulate posterior cortex	178	169	172	152
Precuneus	440	296	342	192

in patients with mTBI. Of particular note, these regions do not belong to the DMN.

Precuneus connectivity map. Using the precuneus as a seed region, the between-group analysis (two-sample *t* test) for $p < 0.05$ shows stronger FC between the precuneus and two clusters in patients compared with healthy controls. The first cluster is in the supramarginal gyrus (BA 40) with 82 voxels; the other cluster has 85 voxels, which includes the BA 8 and the anterior cingulate cortex (BA 32) (Fig. 7). Using a cutoff of $p < 0.01$ did not reveal any significant difference.

Thalamus connectivity map. A between-group comparison (two-sample *t* test) was performed using the thalamus as a seed region. For $p < 0.01$, the patient group showed significantly higher FC with the thalamus than controls in several regions, including the anterior prefrontal cortex (BA 10) in two clusters of 83 and 123 voxels (Fig. 8a) and a cluster of 96 voxels in the supramarginal gyrus (BA 40) (Fig. 8b). This indicates an increased FC of the thalamus network with other regions of the brain.

Amygdala connectivity map. By using the amygdala as a seed region, a between-group comparison ($p < 0.01$) demonstrates significantly increased FC with the left parietal superior cortex in the patient group (cluster size = 104) than the control group (Fig. 9). On the other hand, a one-sample *t* test shows that the healthy controls have higher connectivity within the amygdala. For $p < 0.01$, the FC map of the healthy controls group includes 73 and 67 voxels, while for the patient group, these numbers decrease to 39 and 22 (Fig. 10).

Hippocampal connectivity map. A between-group analysis for the FC map with the hippocampus as the seed region demonstrates significant alteration in the FC of patients with mTBI. For $p < 0.01$, three clusters (cluster sizes of 135, 61, and 52 voxels) are significantly different between the two groups. Figure 11 demonstrates increased FC in the fusiform gyrus and the precuneus (BA 7) and decreased FC in the inferior frontal gyrus in the patient group compared with controls (Fig. 11).

Relationship between FC and neurocognitive data. No significant correlation was found between the neurocognitive tests (SAC scores) and FC data. The largest Pearson correlation value (0.42) was found in the SBA for the PCC between the mean of the correlation value with the dorsal anterior cingulate and the delayed recall test, but it did not reach statistical significance.

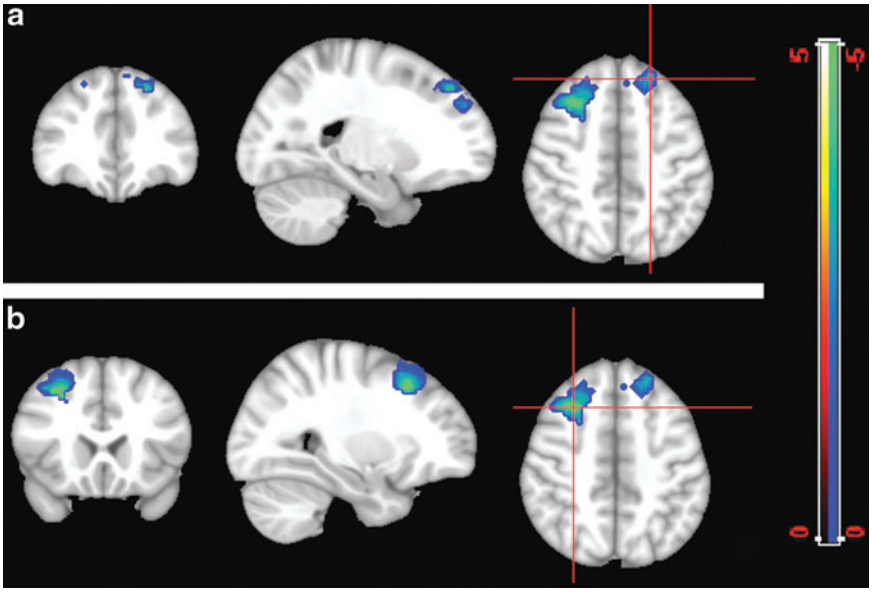

FIG. 6. Two-sample *t* test ($p = 0.01$) for the posterior cingulate cortex functional connectivity (FC) map. The cold color labels the region that has more correlation with the posterior cingulate in the patient group than in the controls. The cross bar is located in different positions in the same FC map in images **a** and **b**. These regions do not belong to the default mode network. Color image is available online at www.liebertpub.com/neu

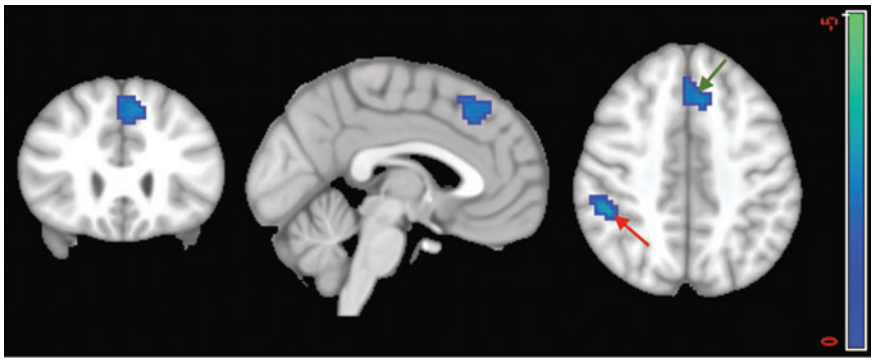

FIG. 7. Two-sample *t* test ($p<0.05$) of the precuneus functional connectivity map. The between group comparison using the precuneus as seed revealed differences in the supramarginal gyrus (red arrow) and the junction between Brodmann area (BA) 8 and the anterior cingulate cortex (BA 32) (green arrow). The cold color labels the regions that have more correlation with the precuneus in the patient group than in controls. Color image is available online at www.liebertpub.com/neu

Discussion

To our knowledge, this is the first investigation of resting-state functional networks in mTBI at the acute stage. Except for one patient who came back for an MRI scan at 7 days after injury, all patients were either still at the ED or in the hospital under observation at the time of scanning. MRI at this point might be the most clinically relevant. Except for one patient with one tiny intraventricular microhemorrhage seen on SWI but not on conventional structural imaging, anatomical imaging did not detect any obvious trauma-induced structural abnormalities in other patients. Both the ICA and SBA, however, revealed differences of brain communication across different brain regions between patients with mTBI and controls in the acute stage. Specifically, a comprehensive analysis showed reduced FC within the DMN and increased functional connectivity with extra-DMN regions in patients with mTBI. By using the thalamus, amygdala, and hippocampus as network regions, analyses revealed increased FC with other brain regions. Overall, our data suggest increased involvement of frontal regions after injury at the acute stage. This result confirmed our original hypothesis on altered FC in these functional networks. Further, our results also showed that independent component and seed-based analyses complement each other.

ICA vs. SBA

Both ICA and SBA are widely used methods in resting-state fMRI analysis. Instead of using one, we performed both in a comprehensive analysis of the DMN and the thalamus network at the resting state. Both our group and individual ICA analyses demonstrated reduced connectivity in the PCC and precuneus regions. This was further validated by our SBA results. It demonstrates that the PCC and precuneus connectivity changes in the DMN might be the most well-validated functional biomarkers of brain injury. Meanwhile, because of functional network remodeling in pathological conditions, analysis of the stereotyped networks in the ICA may not be

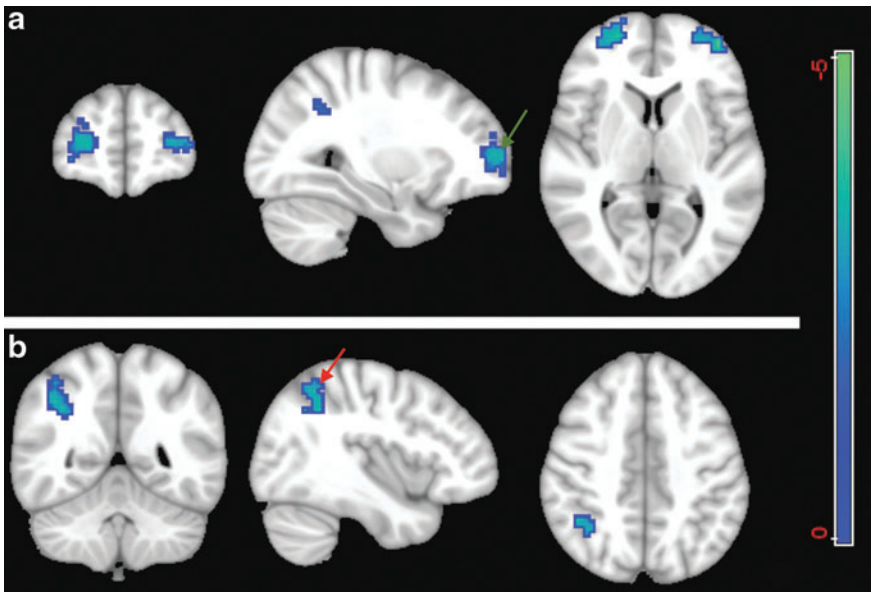

FIG. 8. Two-sample *t* test ($p<0.01$) of thalamus functional connectivity map. The seed is located in the thalamus and the cold color shows the regions that have higher correlation with seed point in the patient group compared with the healthy control group. (**a**) Shows a statistical difference between two groups at the anterior prefrontal cortex (Brodmann area [BA] 10) (green arrow) and (**b**) shows the difference in the supramarginal gyrus (BA 40) (red arrow). Color image is available online at www.liebertpub.com/neu

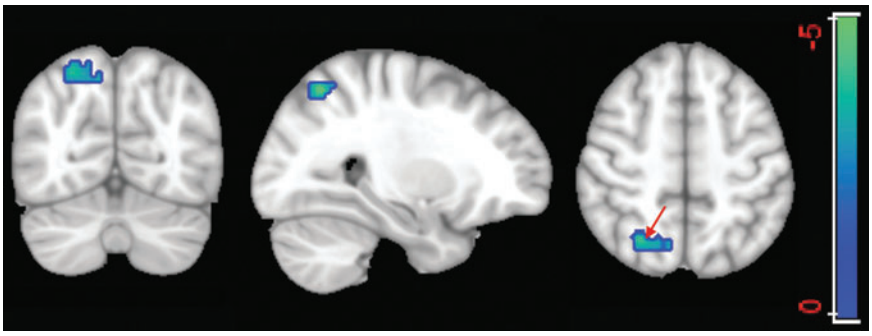

FIG. 9. Two-sample *t* test ($p < 0.01$) for the amygdala correlation map. The cold color labels the region (the left parietal superior cortex) that has stronger correlation with the amygdala (red arrow) in the patient group than in controls. Color image is available online at www.liebertpub.com/neu

able to capture the dynamics of network alterations in mTBI. Instead, SBA demonstrated increased FC in major regions of the DMN, thalamus, amygdala, and hippocampus with other networks of the brain, and this finding further complements the ICA results.

DMN

Our data showed decreased strength of connections and number of voxels involved within the DMN and increased connectivity between the DMN and other brain regions. This result is, in large part, consistent with studies of mTBI at the subacute and chronic stages.[27,28,32] Mayer and associates[27] attributed this abnormality to the partial disruption of the putative balance between the DMN and task-related networks after mTBI, and Stevens and colleagues[32] interpreted this abnormality as a compensatory process of the brain. Palacios and coworkers[48] also attribute this to a compensatory process after microstructural damage to the brain, as detected by DTI. In addition, by considering the hyperconnectivity in thalamocortical network, hippocampal network, and amygdala network, our data also support the hypothesis by Stevens and colleagues[32] that multiple RSNs could have functional abnormalities after mTBI. The brain tends to respond to head injury by recruiting a cohort of networks in a global manner instead of just one or two networks, disrupting the putative balance between resting-state and task-related networks.

The PCC is an important part of the DMN and is also a central hub of the brain.[49] SBA has already reported various connections between the PCC and frontal regions, including the anterior cingulate cortex, orbital frontal cortex, and dorsolateral prefrontal cortex, which are involved in frontal and frontopartial networks.[49–51] Increases in the connectivity between the PCC and these regions were already observed during emotional, memory, and attentional processing.[52,53] A series of cognitive and emotional symptoms have been reported by patients with mTBI in the literature, including anxiety, stress, fear, depression, memory deficits, deficits in problem solving, and difficulty with attention and concentration.[54] Because the PCC receives strong afferent input from regions with functions related to emotional tasks, working memory, and attention including

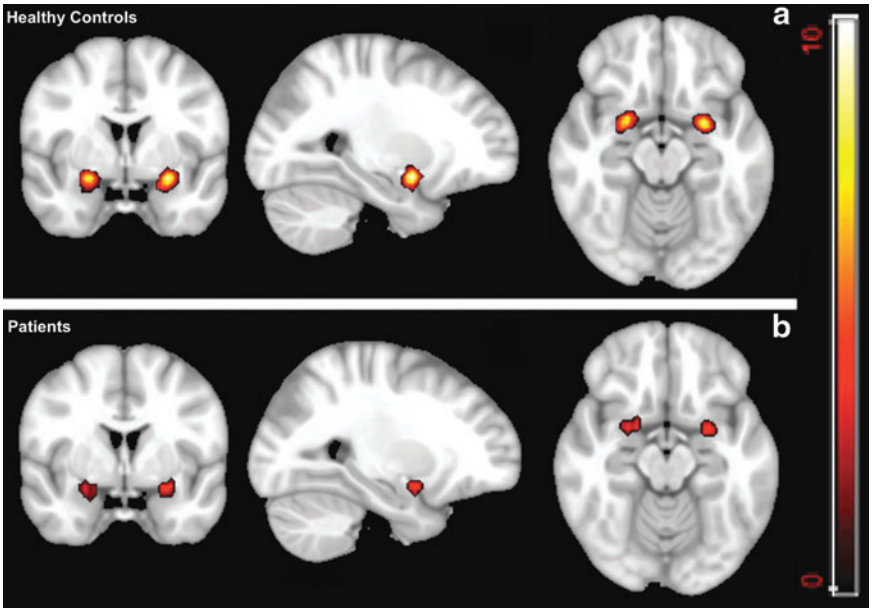

FIG. 10. One-sample *t* test of the amygdala map ($p < 0.01$). (**a**) the functional connectivity (FC) map for the healthy control group and (**b**) the FC map of the patient group. The higher signal intensity on (a) shows higher intrinsic FC in the amygdala in the healthy group than that in patients. Color image is available online at www.liebertpub.com/neu

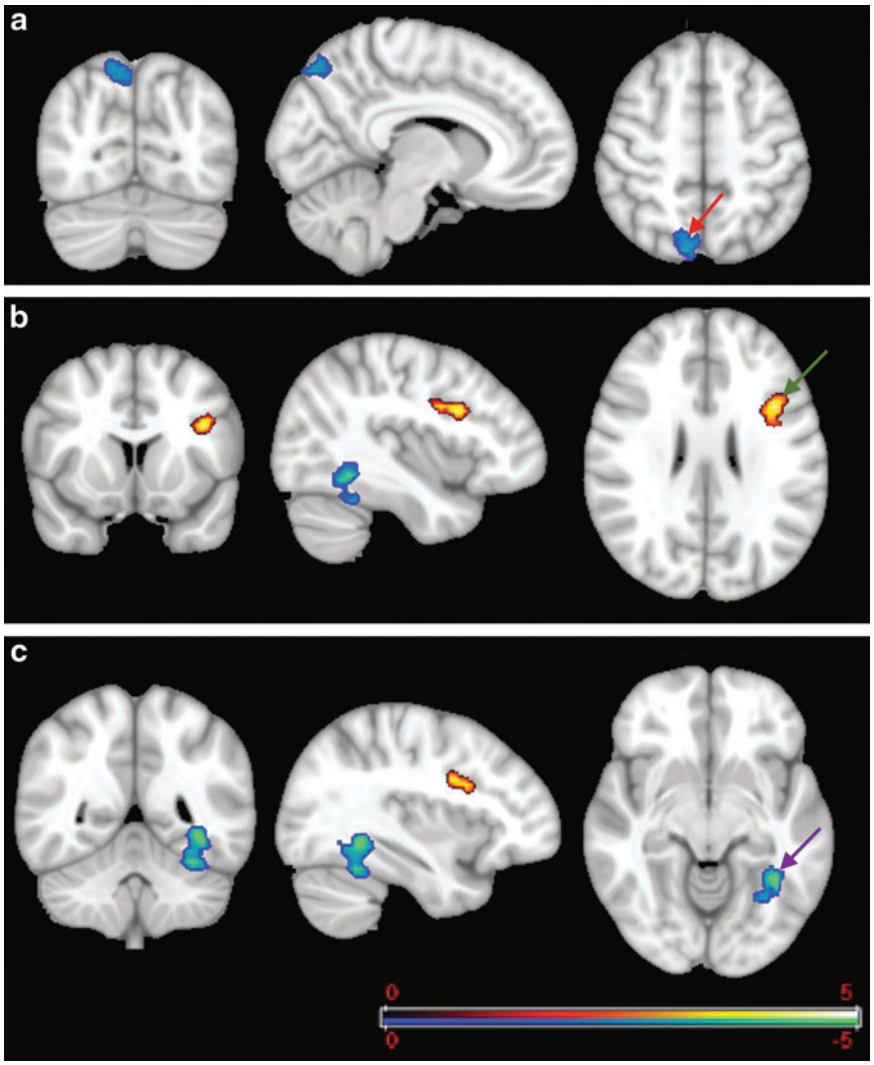

FIG. 11. Two-sample *t* test ($p < 0.01$) for the hippocampus functional connectivity (FC) map. The cold color labels the regions with more correlation with the hippocampus in the patient group compared with controls while the warm color labels the region with more correlation in the controls than in the patient group. The FC map was sectioned through (**a**) the precuneus association cortex (BA 7), red arrow; (**b**) the inferior frontal gyrus, green arrow; and (**c**) the fusiform gyrus, purple arrow.

the anterior cingulate cortex, orbital frontal cortex, and dorsolateral prefrontal cortex (areas 9 and 46),[52,55–59] the cognitive and emotional symptoms after injury could be related to changes in brain networks' activity and connectivity patterns, especially in PCC connectivity.

Our patient group demonstrated significant problems in delayed recall along with the increased connectivity between the PCC and these frontal regions. Further, our ICA results demonstrated a decrease in PCC activity in patients mostly in its ventral part, which is considered the predominant pattern of the DMN.[49] Our data are in line with the reported hypoactivity and hyperfrontality seen in retired National Football League players, as well.[60] This suggests that, right after injury, the PCC might gather information from different brain network regions as an acute compensatory response to bring the brain back to normal status.

One discrepancy between our data and previously reported work is the FC between the PCC and ACC. Previous seed-based studies of mTBI by Mayer and associates[27] and Johnson and coworkers[28] showed reduced FC within the DMN. Both groups showed decreases in FC between the PCC and ACC in the subacute stage while our results showed an increase in temporal correlation between these two regions in the acute stage. One reason for this could be the role of these regions in emotional processing and attention, in association with the temporal resolution. Studies from both groups were at the subacute stage while our study was in the acute stage. With the temporal resolution of patients' PCS, we might see different patterns in the connectivity between the PCC and ACC.

Thalamus FC

The abundance of gamma aminobutyric (GABA)ergic neurons has been thought to play an inhibitory role in the thalamocortical network at resting state.[61,62] Tang and colleagues[37] reported hyperconnectivities in the thalamocortical network in patients with mTBI in suggestion of the disruption of the GABAergic neurons after head injury. Particularly, they reported that the thalamus correlation map in the patient group in the subacute stage is more distributed compared with the healthy control group.[38] Their results show that the healthy subjects' map included areas of the bilateral

thalamus, the superior frontal gyrus, the middle frontal gyrus, the basal ganglia nuclei, the insula, and the cingulate gyrus while patients with mTBI demonstrated more widely distributed FC that extended to the bilateral middle temporal gyrus, the middle frontal gyrus, the precuneus, the inferior parietal gyrus, and the postcentral gyrus compared with the thalamic RSNs in the healthy control subjects ($p < 0.001$, corresponding to $R > 0.25$).

Although our results, unlike their results, showed that all of the active voxels are located in the thalamus for the control group, we got a similar result regarding more distributed correlation maps for the patient group compared with the healthy subject group. Their between-group comparison analysis for $p < 0.01$ shows that regions of the cingulate gyrus, temporal gyrus, and frontal gyrus show more correlation with the thalamus in the patient group compared with the control group. With the same p value, we also find increases in temporal correlation in the anterior prefrontal cortex and the supramarginal gyrus with the thalamus in patients compared with controls. In comparison with the data from Tang and associates,[37] our data also demonstrated an up-regulated thalamocortical network as a response to brain injury.

Memory and hippocampal FC

Our data showed memory deficits (in delayed recall) in patients with mTBI at the acute stage, which is in line with the published data that delayed recall is a sensitive index of neurocognitive measures for mTBI at this stage.[39] Our imaging data revealed that the patient group demonstrated decreased intrinsic connectivity in the inferior frontal gyrus and increased connectivity in the fusiform gyrus and precuneus (BA 7). The reduced connectivity in the inferior frontal region is similar to data from Johnson and coworkers,[28] which also reported reduced connectivity between these regions. Our findings of increased connectivity in the fusiform gyrus and precuneus, however, are in contrast with the report of Johnson and coworkers[28] of decreased connections between the parahippocampal gyrus and the left and right parietal lobes in comparison with controls.

Of particular note, our data are regarding patients who still have memory problems while the data of Johnson and associates[28] were collected after resolution of the symptoms. The difference in imaging findings between the two groups may represent the temporal recovery process of memory after mTBI. It also implies that, after suffering intrinsic connectivity problems of the memory network after a concussion, the brain is trying to recruit other networks to compensate.

Amygdala FC

The amygdala is an important structure of the limbic system, crucial to the processing of emotional fear, sadness, and depression, among others emotions.[63,64] Recent evidence suggests cytoarchitectural and functional subspecialization of its substructural nuclei.[65–68] Three major groups of subnuclei include the laterobasal, centromedial, and superfacial groups.[68] Bzdok and colleagues[64] also reported a relationship between functional subspecialization and its structural nuclei. Therefore, the conventional view of considering the amygdala complex as a single entity has been challenged.[69] After TBI, emotional symptoms are commonly reported as part of PCS constellation. In our study, 4 of 12 patients reported mild to moderate levels of sadness and depression after injury. The reduced connectivity inside the amygdala and increased connectivity of the amygdala with the left parietal superior cortex in our imaging findings might suggest that emotional fear and sadness after TBI could mediate the intranetwork connectivity among different subnuclei groups within the amygdala. As a consequence, the brain tends to recruit other network resources to compensate.

Limitation and future work

Several factors also set the limitation of this study. To draw a more statistically meaningful conclusion, this work should be performed in a large cohort with longitudinal follow-up instead of a handful of patients at one time point. This study demonstrates functional alteration in several brain networks in patients with mTBI in comparison with controls. All comparison was performed at group level instead of single subject level. For individual ICA analysis, the result still has to be compared at group level before we gain a better understanding of the variations in normal. Future work needs to be performed in a large cohort of patients and controls to identify the structural and functional connectivity damages at the single subject level. Further, the question of how RSN alterations affect the patients' neurocognitive performance as measured by PCS and a neuropsychological assessment battery still need to be determined.

Meanwhile, despite the normal findings on structural MRI in these patients, it does not mean they are normal on advanced MRI, including DTI. Mounting evidence demonstrates the microstructural damage in patients with mTBI.[8,70–73] Our pilot data suggest that, in response to microstructural damage on the cingulate bundle shown on DTI, other regions of the brain tend to have higher FC with the anterior cingulate cortex on resting state fMRI signal.[74] This suggests a compensatory mechanism of brain injury. A systematic investigation in a large cohort is warranted in this direction to delineate the brain compensatory mechanism. In addition, our data clearly demonstrate the multinetwork alterations after mTBI, which are in the same line as the work of Stevens and associates.[32] Further advanced DTI data also demonstrate that mTBI could render microstructural damages in multiple WM tracts.[70] This indicates the value of a future connectome-scale analysis of mTBI by combining both DTI and fMRI data to reveal a much more clear picture of brain injury.[74]

It is also worth mentioning that an increase in temporal correlation in different regions of a network does not necessarily indicate an increase in the network activity because the temporal signal of each brain's region consists of several independent time series, which indicate the connection of the region with various brain networks. For instance, although the PCC is well known as a main part of the DMN[75] and has a role in mind wandering, memory recollection, etc., it also has important roles in many other networks such as frontoparietal networks, a motor network, a sensory network, and an executive network.[49,76]

Therefore, it is possible that temporal correlations between the PCC and other brain regions increased while the activity of the DMN decreased, or vice versa, because the time series of each region can be the result of a combination of the temporal activity of several networks. For instance, Leech and associates[49] showed that the PCC consists of several subregions that have separate signals and each contribute to different networks. Although the average signal of these subregions showed high correlation between subregions, the correlation between the neural signal of these subregions was much lower, indicating that, despite having high temporal connectivity, they have tasks in different networks. Therefore, further investigation into the physiological underpinning of these functional network changes is still warranted.

Conclusion

We performed a comprehensive analysis of resting-state DMN and several other networks in patients with acute mTBI. Our study demonstrated multinetwork alterations in mTBI at the acute stage, including decreased intranetwork connectivity and increased internetwork connectivity of the DMN and amygdala network as well as changes in the thalamus and hippocampus networks. Particularly, the DMN alterations could be used as a biomarker for the diagnosis of functional deficit in mTBI in the acute setting. A longitudinal study of large-scale brain networks over a large cohort is also warranted to further reveal the physiological basis of the neurocognitive symptoms of mTBI.

Acknowledgments

This study was supported by the International Society for Magnetic Resonance in Medicine (ISMRM) seed grant and the Department of Defense (grant contract number: W81XWH-11-1-0493). The authors also thank Ms. Natalie Wiseman, MD, PhD candidate, for proofreading.

Author Disclosure Statement

No competing financial interests exist.

References

1. Kay, T. (1993). Neuropsychological treatment of mild traumatic brain injury. J Head Trauma Rehabil. 8, 74–85.
2. National Institutes of Health (1999). Rehabilitation of personswith traumatic brain injury. NIH Consensus Development Panel on Rehabilitation of Persons With Traumatic Brain Injury. JAMA 282, 974–983.
3. CDC (2003). *Report to Congress on Mild Traumatic Brain Injury in the United States: Steps to Prevent a Serious Public Health Problem.* Centers for Disease Control and Prevention, National Center for Injury Prevention and Control: Atlanta, GA.
4. Bazarian, J.J., McClung, J., Cheng, Y.T., Flesher, W., and Schneider, S.M. (2005). Emergency department management of mild traumatic brain injury in the USA. Emerg. Med. J. 22, 473–477.
5. Bazarian, J.J., McClung, J., Shah, M.N., Cheng, Y.T., Flesher, W., and Kraus, J. (2005). Mild traumatic brain injury in the United States, 1998–2000. Brain Inj. 19, 85–91.
6. Ruff, R. (2005). Two decades of advances in understanding of mild traumatic brain injury. J. Head Trauma Rehabil. 20, 5–18.
7. Jagoda, A.S., Bazarian, J.J., Bruns, J.J., Jr., Cantrill, S.V., Gean, A.D., Howard, P.K., Ghajar, J., Riggio, S., Wright, D.W., Wears, R.L., Bakshy, A., Burgess, P., Wald, M.M., and Whitson, R.R. (2008). Clinical policy: neuroimaging and decisionmaking in adult mild traumatic brain injury in the acute setting. Ann. Emerg. Med. 52, 714–748.
8. Kou, Z., Wu, Z., Tong, K.A., Holshouser, B., Benson, R.R., Hu, J., and Haacke, E.M. (2010). The role of advanced MR imaging findings as biomarkers of traumatic brain injury. J. Head Trauma Rehabil. 25, 267–282.
9. Kou, Z., Benson, R.R., and Haacke, E. M. (2012). Magnetic resonance imaging biomarkers of mild traumatic brain injury, in: *Biomarkers for Traumatic Brain Injury*. S.A. Dambinova, R.L. Hayes, K.K. Wang (eds). Royal Society of Chemistry: Cambridge, UK.
10. Shimony, J.S., McKinstry, R.C., Akbudak, E., Aronovitz, J.A., Snyder, A.Z., Lori, N.F., Cull, T.S., and Conturo, T.E. (1999). Quantitative diffusion-tensor anisotropy brain MR imaging: normative human data and anatomic analysis. Radiology 212, 770–784.
11. Conturo, T.E., McKinstry, R.C., Akbudak, E., and Robinson, B.H. (1996). Encoding of anisotropic diffusion with tetrahedral gradients: a general mathematical diffusion formalism and experimental results. Magn. Res. Med. 35, 399–412.
12. Mac Donald, C.L., Dikranian, K., Song, S.K., Bayly, P.V., Holtzman, D.M. and Brody, D.L. (2007). Detection of traumatic axonal injury with diffusion tensor imaging in a mouse model of traumatic brain injury. Exp. Neurol. 205, 116–131.
13. Kou, Z., Shen, Y., Zakaria, N., Kallakuri, S., Cavanaugh, J.M., Yu, Y., Hu J., and EM, H. (2007). Correlation of fractional anisotropy with histology for diffuse axonal injury in a rat model. Proceedings of the Joint Annual Meeting ISMRM-ESMRMB: Berlin, Germany.
14. Ptak, T., Sheridan, R.L., Rhea, J.T., Gervasini, A.A., Yun, J.H., Curran, M.A., Borszuk, P., Petrovick, L., and Novelline, R.A (2003). Cerebral fractional anisotropy score in trauma patients: a new indicator of white matter injury after trauma. AJR Am. J. Roentgenol. 181, 1401–1407.
15. Huisman, T.A., Schwamm, L.H., Schaefer, P.W., Koroshetz, W.J., Shetty-Alva, N., Ozsunar, Y., Wu, O., and Sorenson, A.G. (2004). Diffusion tensor imaging as potential biomarker of white matter injury in diffuse axonal injury. AJNR Am. J. Neuroradiol. 25, 370–376.
16. Arfanakis, K., Haughton, V.M., Carew, J.D., Rogers, B.P., Dempsey, R.J., and Meyerand, M.E. (2002). Diffusion tensor MR imaging in diffuse axonal injury. AJNR Am. J. Neuroradiol. 23, 794–802.
17. Inglese, M., Makani, S., Johnson, G., Cohen, B.A., Silver, J.A., Gonen, O., and Grossman, R.I. (2005). Diffuse axonal injury in mild traumatic brain injury: a diffusion tensor imaging study. J. Neurosurg. 103, 298–303.
18. Benson, R.R., Meda, S.A., Vasudevan, S., Kou, Z., Govindarajan, K.A., Hanks, R.A., Millis, S.R., Makki, M., Latif, Z., Coplin, W., Meythaler, J., and Haacke, E.M. (2007). Global white matter analysis of diffusion tensor images is predictive of injury severity in traumatic brain injury. J. Neurotrauma 24, 446–459.
19. Mac Donald, C.L., Johnson, A.M., Cooper, D., Nelson, E.C., Werner, N.J., Shimony, J.S., Snyder, A.Z., Raichle, M.E., Witherow, J.R., Fang, R., Flaherty, S.F., and Brody, D.L. (2011). Detection of blast-related traumatic brain injury in U.S. military personnel. N. Engl. J. Med. 364, 2091–2100.
20. Kou, Z., Benson, R.R., and Haacke, E.M. Susceptibility weighted imaging in traumatic brain injury, in: *Clinical MR Neuroimaging,* 2nd ed. J. Gillard, A. Waldman, P. Barker (eds). Cambridge University: Cambridge, UK.
21. Paterakis, K., Karantanas, A.H., Komnos, A., and Volikas, Z. (2000). Outcome of patients with diffuse axonal injury: the significance and prognostic value of MRI in the acute phase. J Trauma 49, 1071–1075.
22. Reichenbach, J.R., Venkatesan, R., Schillinger, D.J., Kido, D.K., and Haacke, E.M. (1997). Small vessels in the human brain: MR venography with deoxyhemoglobin as an intrinsic contrast agent. Radiology 204, 272–277.
23. McAllister, T.W., Flashman, L.A., McDonald, B.C., and Saykin, A.J. (2006). Mechanisms of working memory dysfunction after mild and moderate TBI: evidence from functional MRI and neurogenetics. J Neurotrauma 23, 1450–1467.
24. Yang, Z., Yeo, R.A., Pena, A., Ling, J.M., Klimaj, S., Campbell, R., Doezema, D, and Mayer, A.R. (2012). An FMRI study of auditory orienting and inhibition of return in pediatric mild traumatic brain injury. J. Neurotrauma 29, 2124–2136.
25. Keightley, M.L., Saluja, R.S., Chen, J.K., Gagnon, I., Leonard, G., Petrides, M., and Ptito, A. (2014). A functional magnetic resonance imaging study of working memory in youth after sports-related concussion: is it still working? J. Neurotrauma 31, 437–451.
26. Dettwiler, A., Murugavel, M., Putukian, M., Cubon, V., Furtado, J., and Osherson, D. (2014). Persistent differences in patterns of brain activation after sports-related concussion: a longitudinal functional magnetic resonance imaging study. J. Neurotrauma 31, 180-–88.
27. Mayer, A.R., Mannell, M.V., Ling, J., Gasparovic, C., and Yeo, R.A. (2011). Functional connectivity in mild traumatic brain injury. Hum Brain Mapp 32, 1825–1835.
28. Johnson, B., Zhang, K., Gay, M., Horovitz, S., Hallett, M., Sebastianelli, W., and Slobounov, S. (2012). Alteration of brain default network in subacute phase of injury in concussed individuals: resting-state fMRI study. Neuroimage 59, 511–518.
29. Wang, L., Zang, Y.F., He, Y., Liang, M., Zhang, X.Q., Tian, L.X., Wu, T., Jiang, T.Z. and Li, K.C. (2006). Changes in hippocampal connectivity in the early stages of Alzheimer's disease: evidence from resting state fMRI. Neuroimage 31, 496–504.
30. Zhou, Y., Liang, M., Tian, L.X., Wang, K., Hao, Y.H., Liu, H.H., Liu, Z.N., and Jiang, T.Z. (2007). Functional disintegration in

paranoid schizophrenia using resting-state fMRI. Schizophr. Res. 97, 194–205.
31. Tian, L.X., Jiang, T.Z., Wang, Y.F., Zang, Y.F., He, Y., Liang, M., Sui, M.Q., Cao, Q.J., Hu, S.Y., Peng, M., and Zhuo, Y. (2006). Altered resting-state functional connectivity patterns of anterior cingulate cortex in adolescents with attention deficit hyperactivity disorder. Neurosci. Lett. 400, 39–43.
32. Stevens, M.C., Lovejoy, D., Kim, J., Oakes, H., Kureshi, I. and Witt, S.T. (2012). Multiple resting state network functional connectivity abnormalities in mild traumatic brain injury. Brain imaging and behavior 6, 293–318.
33. Zhang, K., Johnson, B., Gay, M., Horovitz, S.G., Hallett, M., Sebastianelli, W., and Slobounov, S. (2012). Default mode network in concussed individuals in response to the YMCA physical stress test. J. Neurotrauma 25, 756–765.
34. Broyd, S.J., Demanuele, C., Debener, S., Helps, S.K., James, C.J., and Sonuga-Barke, E.J. (2009). Default-mode brain dysfunction in mental disorders: a systematic review. Neurosci. Biobehav. Rev. 33, 279–296.
35. Binder, J.R., and Desai, R.H. (2011). The neurobiology of semantic memory. Trends Cogn. Sci. 15, 527–536.
36. Gilbert, S.J., Dumontheil, I., Simons, J.S., Frith, C.D., and Burgess, P.W. (2007). Comment on ''Wandering minds: The default network and stimulus-independent thought''. Science 317, 43.
37. Tang, L., Ge, Y., Sodickson, D.K., Miles, L., Zhou, Y., Reaume, J., and Grossman, R.I. (2011). Thalamic resting-state functional networks: disruption in patients with mild traumatic brain injury. Radiology 260, 831–840.
38. McCrea, M.A. (2008). *Mild Traumatic Brain Injury and Postconcussion Syndrome*. Oxford University Press: New York, NY.
39. Naunheim, R.S., Matero, D, and Fucetola, R. (2008). Assessment of patients with mild concussion in the emergency department. J. Head Trauma Rehabil. 23, 116–122.
40. American Congress of Rehabilitation Medicine (1993). Definition of mild traumatic brain injury. J. Head Trauma Rehabil. 8, 86–88.
41. McCrea, M., Randolph, C., and Kelly, J.P. (2000). *Standardized Assessment of Concussion (SAC): Manual for Administration, Scoring and Interpretation,* 2nd ed. CNS Inc.: Waukesha, WI.
42. McCrea, M., Guskiewicz, K.M., Marshall, S.W., Barr, W., Randolph, C., Cantu, R.C., Onate, J.A., Yang, J., and Kelly, J.P. (2003). Acute effects and recovery time following concussion in collegiate football players: the NCAA Concussion Study. JAMA 290, 2556–2563.
43. Beckmann, C.F., Mackay, C.E., Filippini, N., and Smith, S.M. (2009). Group comparison of resting-state FMRI data using multi-subject ICA and dual regression. Neuroimage 47, S148.
44. Calhoun, V.D., Adali, T., Pearlson, G.D., and Pekar, J.J. (2001). A method for making group inferences from functional MRI data using independent component analysis. Hum. Brain Mapp. 14, 140–151.
45. Allen, E.A., Erhardt, E.B., Damaraju, E., Gruner, W., Segall, J.M., Silva, R.F., Havlicek, M., Rachakonda, S., Fries, J., Kalyanam, R., Michael, A.M., Caprihan, A., Turner, J.A., Eichele, T., Adelsheim, S., Bryan, A.D., Bustillo, J., Clark, V.P., Feldstein Ewing, S.W., Filbey, F., Ford, C.C., Hutchison, K., Jung, R.E., Kiehl, K.A., Kodituwakku, P., Komesu, Y.M., Mayer, A.R., Pearlson, G.D., Phillips, J.P., Sadek, J.R., Stevens, M., Teuscher, U., Thoma, R.J. and Calhoun, V.D. (2011). A baseline for the multivariate comparison of resting-state networks. Front. Syst. Neurosci. 5, 2.
46. Lin, Q.H., Liu, J., Zheng, Y.R., Liang, H., and Calhoun, V.D. (2010). Semiblind spatial ICA of fMRI using spatial constraints. Hum. Brain Mapp. 31, 1076–1088.
47. McCrea, M., Kelly, J.P., Randolph, C., Kluge, J., Bartolic, E., Finn, G., and Baxter, B. (1998). Standardized assessment of concussion (SAC): on-site mental status evaluation of the athlete. J. Head Trauma Rehabil. 13, 27–35.
48. Palacios, E.M., Sala-Llonch, R., Junque, C., Roig, T., Tormos, J.M., Bargallo, N., and Vendrell, P. (2013). Resting-state functional magnetic resonance imaging activity and connectivity and cognitive outcome in traumatic brain injury. JAMA Neurol. 70, 845–851.
49. Leech, R., Braga, R., and Sharp, D.J. (2012). Echoes of the brain within the posterior cingulate cortex. J. Neurosci. 32, 215–222.
50. Koechlin, E., Ody, C., and Kouneiher, F. (2003). The architecture of cognitive control in the human prefrontal cortex. Science 302, 1181–1185.
51. Koechlin, E., and Summerfield, C. (2007). An information theoretical approach to prefrontal executive function. Trends Cogn. Sci. 11, 229–235.
52. Maddock, R.J., Garrett, A.S., and Buonocore, M.H. (2003). Posterior cingulate cortex activation by emotional words: fMRI evidence from a valence decision task. Hum. Brain Mapp. 18, 30–41.
53. Maratos, E.J., Dolan, R.J., Morris, J.S., Henson, R.N., and Rugg, M.D. (2001). Neural activity associated with episodic memory for emotional context. Neuropsychologia 39, 910–920.
54. Bergman, K., and Bay, E. (2010). Mild traumatic brain injury/concussion: a review for ED nurses. J. Emerg. Nurs. 36, 221–230.
55. Allison, T., Puce, A., and McCarthy, G. (2000). Social perception from visual cues: role of the STS region. Trends Cogn. Sci. 4, 267–278.
56. Carmichael, S.T., and Price, J.L. (1995). Limbic connections of the orbital and medial prefrontal cortex in macaque monkeys. J. Comp. Neurol. 363, 615–641.
57. Goldman-Rakic, P.S., Selemon, L.D. and Schwartz, M.L. (1984). Dual pathways connecting the dorsolateral prefrontal cortex with the hippocampal formation and parahippocampal cortex in the rhesus monkey. Neuroscience 12, 719–743.
58. Morris, R., Pandya, D.N., and Petrides, M. (1999). Fiber system linking the mid-dorsolateral frontal cortex with the retrosplenial/presubicular region in the rhesus monkey. J. Comp. Neurol. 407, 183–192.
59. Pandya, D.N., Van Hoesen, G.W. and Mesulam, M.M. (1981). Efferent connections of the cingulate gyrus in the rhesus monkey. Exp. Brain Res. 42, 319–330.
60. Hampshire, A., MacDonald, A., and Owen, A.M. (2013). Hypoconnectivity and hyperfrontality in retired American football players. Sci. Rep. 3, 2972.
61. Aron, A.R., Schlaghecken, F., Fletcher, P.C., Bullmore, E.T., Eimer, M., Barker, R., Sahakian, B.J., and Robbins, T.W. (2003). Inhibition of subliminally primed responses is mediated by the caudate and thalamus: evidence from functional MRI and Huntington's disease. Brain 126, 713–723.
62. Steriade, M. (2005). Sleep, epilepsy and thalamic reticular inhibitory neurons. Trends Neurosci. 28, 317–324.
63. Morris, J.S., Frith, C.D., Perrett, D.I., Rowland, D., Young, A.W., Calder, A.J., and Dolan, R.J. (1996). A differential neural response in the human amygdala to fearful and happy facial expressions. Nature 383, 812–815.
64. Bzdok, D., Laird, A.R., Zilles, K., Fox, P.T., and Eickhoff, S.B. (2013). An investigation of the structural, connectional, and functional subspecialization in the human amygdala. Hum. Brain Mapp. 34, 3247–3266.
65. Adolphs, R. (2008). Fear, faces, and the human amygdala. Curr. Opin. Neurobiol. 18, 166–172.
66. Adolphs, R. (2010). What does the amygdala contribute to social cognition? Ann. N. Y. Acad. Sci. 1191, 42–61.
67. LeDoux, J.E. (2000). Emotion circuits in the brain. Ann. Rev. Neurosci. 23, 155–184.
68. Amunts, K., Kedo, O., Kindler, M., Pieperhoff, P., Mohlberg, H., Shah, N.J., Habel, U., Schneider, F., and Zilles, K. (2005). Cytoarchitectonic mapping of the human amygdala, hippocampal region and entorhinal cortex: intersubject variability and probability maps. Anat Embryol (Berl) 210, 343–352.
69. Swanson, L.W., and Petrovich, G. (1998). What is the amygdala? Trends Neurosci. 21, 323–331.
70. Kou, Z., and VandeVord, P.J. (2014). Traumatic white matter injury and glial activation: from basic science to clinics. Glia 62, 1831–1855.
71. Kou, Z., Gattu, R., Kobeissy, F., Welch, R.D., O'Neil, B., Woodard, J.L., Ayaz, S.I., Kulek, A., Kas-Shamoun, R., Mika, V., Zuk, C., Hayes, R.L., Tomasello, F., and Mondello, S. (2013). Combining biochemical and imaging markers to improve diagnosis and characterization of mild traumatic brain injury in the acute setting: results from a pilot study. PLoS One 8, e80296.
72. Niogi, S.N., and Mukherjee, P. (2010). Diffusion tensor imaging of mild traumatic brain injury. J. Head Trauma Rehabil. 25, 241–255.
73. Niogi, S.N., Mukherjee, P., Ghajar, J., Johnson, C.E., Kolster, R., Lee, H., Suh, M., Zimmerman, R.D., Manley, G.T., and McCandliss, B.D. (2008). Structural dissociation of attentional control and memory in adults with and without mild traumatic brain injury. Brain 131, 3209–3221.

74. Kou, Z., and Iraji, A. (2014). Imaging brain plasticity after trauma. Neural Regen. Res. 9, 693–700.
75. Raichle, M.E., MacLeod, A.M., Snyder, A.Z., Powers, W.J., Gusnard, D.A., and Shulman, G.L. (2001). A default mode of brain function. Proc. Natl. Acad. Sci. U.S.A. 98, 676–682.
76. Pearson, J.M., Heilbronner, S.R., Barack, D.L., Hayden, B.Y., and Platt, M.L. (2011). Posterior cingulate cortex: adapting behavior to a changing world. Trends Cogn. Sci. 15, 143–151.

Address correspondence to:
Zhifeng Kou, PhD
Department of Biomedical Engineering
Wayne State University
Detroit, MI 48201

E-mail: Zhifeng_kou@wayne.edu